P6M.4

SIMULATED PRECIPITATION STRUCTURE OF THE EXTRATROPICAL TRANSITION OF TROPICAL CYCLONES

Elizabeth A. Ritchie*
University of New Mexico, Albuquerque, NM.

1. INTRODUCTION

The second, or *reintensification,* stage of the extratropical transition (ET) of tropical cyclones occurs when a transformed tropical cyclone re-intensifies if the midlatitude conditions are favorable for extratropical cyclogenesis, which is usually as part of an interaction with a midlatitude upper-level trough (e.g., DiMego and Bosart 1982, Harr and Elsberry 2000, Klein et al. 2000). Klein et al. (2000) noted in their study of 30 western North Pacific ET events that this *re-intensification* stage was very dependent on the details of the midlatitude circulation structure and how the transformed tropical cyclone interacted with that midlatitude circulation. In particular, poleward-moving tropical cyclones underwent a variety of re-intensification rates. Of those that did significantly re-intensify, the ability of forecast models to accurately predict the rate of intensification and future track of the storm was at times poor, with large discrepancies from forecast to forecast even by the same model (P. Harr 2000; personal communication). This led to the Harr and Elsberry (2000) hypothesis that the details of the structure of the transformed tropical cyclone has relatively little influence on the intensification processes; rather, it is the structure of the midlatitude environment that determines the rate and nature of re-intensification. If the forecast model poorly handles the timing of the transformed tropical cyclone with the midlatitude environment, a poor re-intensification forecast results.

Prior studies of ET (DiMego and Bosart 1982, Sinclair 1993, Foley and Hanstrum 1994, Harr and Elsberry 2000, Harr et al. 2000) have described reintensification of the transformed tropical cyclone in terms of a Type-B development following Petterssen and Smebye (1971). In this context, low-level cyclone development occurs when an area of mid-level positive vorticity advection (PVA) becomes superposed over a low-level frontal region, allowing low-level thermal advection to contribute significantly to an increase in low-level vorticity. When the thermal field is distorted through circular motion, as may occur during transformation of a tropical cyclone (Klein et al. 2000), the thermal contribution becomes significant (Petterssen 1956). In this framework, the phasing of the tropical cyclone remnants with the upper-level trough clearly should be the key factor in determining whether the low-level and upper-level components of Type-B development are properly superposed during the reintensification of the extratropical cyclone.

Ritchie and Elsberry (2003) studied the relationship between the strength of the upper-level trough and subsequent reintensification without changing the phasing between the two weather systems. In their idealized simulations, the strength of the upper-level trough had little impact on the final intensity of the extratropical cyclone, but did impact the rate at which the intensification occurred. Of note was their conclusion that the basic structure of the midlatitude environment may have more to do with the final intensity of the extratropical cyclone than the strength of the upper-level trough embedded within that environment as their basic environment was the same for all simulations.

The purpose of this study is to continue to investigate the interaction between the midlatitude upper-level trough and tropical cyclone during the re-intensification stage of ET. In particular, the effects of altering the phasing between the upper-level, midlatitude trough and the tropical cyclone are investigated. Following Ritchie and Elsberry (2003), a series of simulations are performed using the Navy's Coupled Ocean-Atmospheric Mesoscale Prediction System (COAMPS) to investigate how different phasing between a midlatitude upper-level trough and the tropical cyclone impact the subsequent reintensification of the extratropical cyclone. As noted in Klein et al. (2002), changing the relative location of the systems by only a small amount can dramatically affect the subsequent interaction. Specifically, this study differs from that of Klein et al. (2002) and McTaggart-Cowan et al. (2001) in that it directly examines the effect of

*Corresponding Author Address: Elizabeth Ritchie, ECE Building, Room 125, University of New Mexico, Albuquerque, NM 87131. email: ritchie@ece.unm.edu

modifying the phasing between the upper-level trough and the tropical cyclone without changing the specific characteristics of either weather system as an intermediate step to understanding the re-intensification stage of the ET of a tropical cyclone.

The structure of the paper will be as follows. A description of the modeling system and experimental setup will be provided in section 2. The consequences of altering the phasing between the upper-level trough and tropical cyclone will be discussed in section 3. A comparison of the major differences that produce dissipating systems as opposed to moderate or deeply re-intensifying systems will be provided in section 4. A preliminary parameter identifier for whether a system will dissipate or reintensify is discussed in section 5. A summary and conclusions are provided in section 6.

2. Description of the modeling system

High-resolution idealized simulations of ET will be studied here using only the atmospheric portion of COAMPS (Hodur 1997). The advantage of simulations using such a modeling system is that the varying atmospheric conditions among cases can be controlled.

2.1 Model description

The COAMPS model employed in the study is described in detail by Hodur (1997). The system is nonhydrostatic, has multiple nested grids, and includes a Kain-Fritsch (Kain and Fritsch 1993) representation of convection, and explicit moist physics (Rutledge and Hobbs 1983) for grid-scale saturation. Additional parameterizations include sub-grid scale mixing (Deardorff 1980), surface fluxes (Louis 1979), and radiation (Harshvardhan et al. 1987). The primitive equations are solved on a Lambert conformal grid, with a terrain-following σ-coordinate in the vertical. The model has 36 layers from σ=0 to 1, with the vertical boundaries at 30 km and the surface. Whereas vertical velocity is defined at the interfaces of the model layers, all other variables are carried at the mid-points of the layers. The horizontal grid has an Arakawa-Lamb C-staggering of the momentum variables (u and v) with respect to the other variables.

The configuration used for these simulations is the same as that for Ritchie and Elsberry (2003) and are described there. Briefly, the coarse and fine meshes have grid spacings of 81 km and 27 km, respectively. The coarse domain of 87 x 93 grid points is large enough to allow an adequate representation of the upper-level midlatitude trough development during the integration. The fine mesh of 124 x 190 grid points captures the primary structural modifications of the storm as it interacts with the upper-level trough. The coarse grid supplies boundary values to the fine mesh, which in turn feeds information back to the coarse grid after the fine mesh integration step is completed. The two-way interaction ensures that the fine mesh structure is well represented on the coarse mesh. Lateral boundary conditions (Perkey and Krietzberg 1976) around the coarse domain force the model-predicted variables near the outer boundary to adjust to the fixed initial values.

2.2 Experimental setup

The initial environmental wind vertical structure is the same as that used in Ritchie and Elsberry (2003, 2005) and is based on composite data of western North Pacific ET cases (Ritchie and Elsberry 2001). The horizontal variation in the environmental wind is based on a Gaussian distribution that results in a jet in the wind field near 47°N (not shown). Given this wind structure, the corresponding mass and temperature fields are derived to be in geostrophic and hydrostatic balance, with the mean thermal sounding specified as the composite pre-tropical depression sounding of McBride and Zehr (1981). Although geography is included in figures to help orient the reader, these are idealized simulations in which the entire domain is over ocean. A time-invariant sea-surface temperature gradient is specified to match the near-surface air temperature gradient so that surface fluxes of moisture and heat do not erode the near-surface temperature structure through the simulation. The McBride and Zehr (1981) composite vertical profile of relative humidity is specified everywhere so that the meridional temperature gradient implies moist (dry) air to the south (north). A balanced upper-level potential vorticity perturbation with a Gaussian vertical wind structure maximum at 380 mb then is added to this environment to represent the midlatitude upper-level trough. The resulting upper-level jet streak has a maximum wind speed of 50 m s^{-1} at 250 mb.

The initialization of the tropical cyclone is the same as in Ritchie and Elsberry (2001, 2003, 2005). The tropical cyclone is spun up in a quiescent environment until an approximately steady-state intensity of 960 mb is reached and the cloud fields are fully developed. This initial tropical cyclone has a maximum wind of 55 m s^{-1} at a radius of 70 km. The core structure is approximately symmetric with cyclonic winds extending to 50 mb in the core and a maximum temperature anomaly of

12 K at 450 mb. The 300-mb winds turn weakly anticyclonic at 400 km radius.

The initial conditions for 16 simulations are created by inserting the tropical cyclone into the environment every 5 degrees latitude/10 degrees longitude in a 4 x 4 grid (Fig. 1). The closest location to the trough is 10 degrees south and 15 degrees east of the trough, and the farthest location is 25 degrees south and 45 degrees east of the trough (Fig. 1). All simulations are integrated for 192 h. By this time the original trough has advected out of the domain, and any subsequent development is due to interaction with the *in situ* development of a secondary trough.

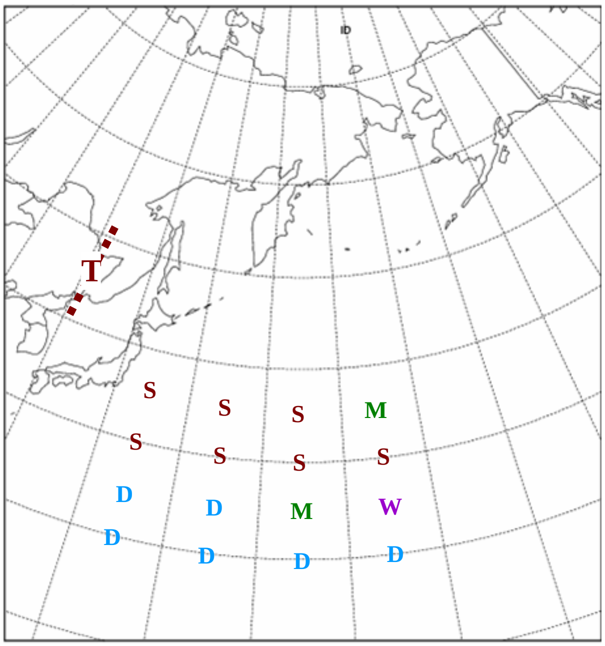

Fig. 1: Schematic indicating the initial positions of the TC relative to the upper-level trough (T) and the final intensities extratropical cyclone reached. Classifications are S = strong intensifier, M = moderate intensifier, and D = dissipator.

3. THE PHASING BETWEEN THE UPPER-LEVEL TROUGH AND TROPICAL CYCLONE

The evolution of the minimum sea-level pressure (slp) associated with each simulation is shown in Fig. 2. The final pressures can be clustered into three re-intensification groups that are similar to those defined by Klein et al. (2000): non/weak (N/W: slp > 1000 mb), moderate (M: 975 mb < slp < 999 mb), and strong (S: slp < 975 mb) intensifiers. In these idealized simulations, the different evolutions must be due to differences in the interaction between the midlatitude trough and tropical cyclone arising only from the relative positions in Fig. 1. Thus, the final intensity achieved by the system in Fig. 2 is strongly dependent on the relative positioning of the tropical cyclone and midlatitude trough (Fig. 1). In general, those cases in which the tropical cyclone is initially closest to the baroclinic zone and upper-level trough (within 15º latitude) develop the deepest intensities and those farthest away (20º-25º south of the trough) are more likely to dissipate or only weakly re-intensify. However, the re-intensification varies with the initial longitudinal position as well. The strong re-intensification for the tropical cyclone initially at 15°S and 45°E appears anomalous relative to the moderate values at 10°S and 45°E and 20°S and 35°E.

The reasons for these evolutions may be sought in the tropical cyclone paths relative to the baroclinic zone associated with the upper-level trough. The tropical cyclones initially closest to the baroclinic zone tracked northeast immediately into and across the baroclinic zone (Fig. 3), which is expected as they were advected by the northeasterly flow ahead of the upper-level trough. The tropical cyclones that dissipated had a stronger eastward component to their track (Fig. 3). By the time these tropical cyclones approached and crossed the baroclinic zone, the upper-level trough had already passed to the east. Instead of interacting with the trough, these tropical cyclones were advected by the westerlies associated with the background baroclinic zone and moved rapidly eastward as they dissipated in the environmental vertical wind shear. Note that

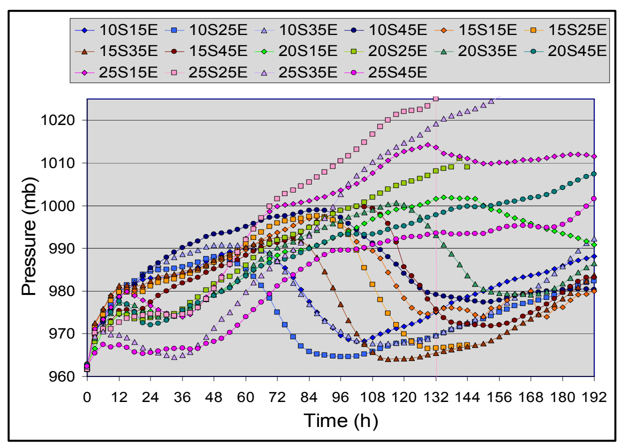

Fig. 2: *Time series of the minimum surface pressure for all 16 simulations color-coded by latitudinal location.*

the spatial patterning did not apply to the southeastern-most series of simulations. In these cases (Figs.1, 3), the initial 5 m s^{-1} advection to

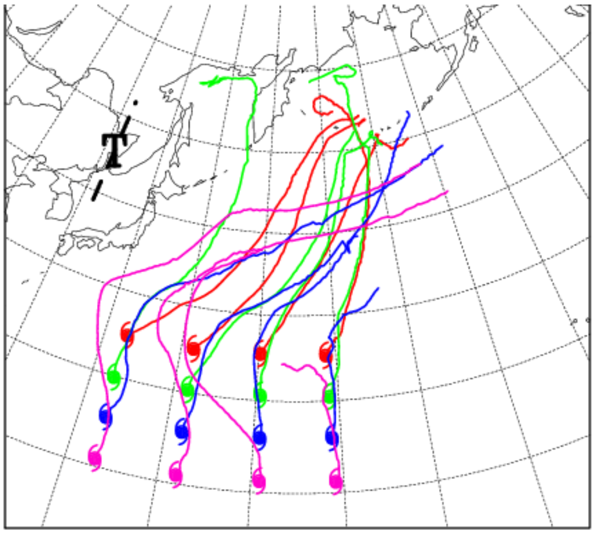

Fig. 3: *Tracks all 16 cases showing the two distinct types of tracks – more northward for the systems located closer to the trough and more eastward for the systems generally located farther south of the trough. Red = 10°S, Green = 15°S, Blue = 20°S, and pink = 25°S.*

the northeast added to the tropical cyclone did not advect the tropical cyclone into the midlatitude westerlies before the trough had passed by. These two cases gradually weakened and eventually dissipated.

In summary, the dependency on the initial position of the tropical cyclone highlights the complexity of the phasing between the tropical cyclone and trough for future intensification. In fact, this series of simulations suggests that the phasing between the tropical cyclone and midlatitude trough may be the single most important factor in accurately predicting future intensification trends of a transitioning cyclone in numerical weather prediction models.

4. EXTRATROPICAL TRANSITION

In this section, two representative simulations are examined in some detail to highlight the main differences that occur between a dissipating tropical cyclone and an intensifying tropical cyclone during extratropical transition.

4.1 Re-intensifiers- Case 15S35E

The 500-mb geopotential height and sea-level pressure patterns are presented in Fig. 4 at key stages in the life cycle of a re-intensifying extratropical transition case. Initially the midlatitude trough and the tropical cyclone are distinct features in the 500-mb height and surface pressure fields (Fig. 4a). Prior to 72 h of integration, the tropical cyclone weakens considerably as it approaches the midlatitude baroclinic zone with increasing midlatitude vertical wind shear and lower SSTs (Fig. 2). By 72 h (Fig. 4b), the tropical cyclone has become embedded in the midlatitude trough in the 500-mb fields as an open wave. Although it does still have a distinct surface center in the sea-level pressure field, it has filled to almost its highest central sea-level pressure, which corresponds to the end of stage 1 of extratropical transition as defined by Klein et al. (2000). Subsequent to 72 h of integration, the system enters stage 2 of extratropical transition and begins to reintensify (Fig. 2). During this time, the system is tilted to the west with height (not shown) similar to many documented cases of ET (e.g., DiMego and Bosart 1982). The extratropical cyclone reaches a final intensity of 964 mb in Fig. 4c, and is beginning to occlude.

The 850-mb temperature maps that correspond to the boxed areas in Fig. 4 are presented in Fig. 5. Initially the temperatures exceeding 22°C are concentrated in the core of the TC (Fig. 5a). The strong temperature gradient associated with the baroclinic zone is to the north of the TC. By the end of stage 1, the tropical cyclone has moved into the baroclinic zone and the circulation associated with the tropical cyclone has distorted the temperature gradient so that colder (warmer) air has advected to the west (east) of the tropical cyclone center (Fig. 5b). In addition, frontal regions have developed with a strong warm front to the northeast and a weak cold front to the west of the tropical cyclone center. By the end of stage 2 (Fig. 5c), the core of the cyclone is completely surrounded by sub-freezing air and it has become occluded.

The 6-hourly precipitation maps that correspond to the images in Fig. 4 are presented in Fig. 6. Initially the precipitation is concentrated around the tropical cyclone center and is due to

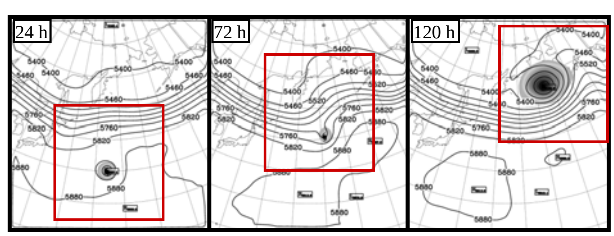

Fig. 4: *500-mb geopotential height field (contour=60m) and sea-level pressure (shaded every 4 mb < 1000 mb) for the intensifying case: a) 24 h; b) end of stage 1; and c) end of stage 2. The boxes indicate the domains for Figs. 5 and 6.*

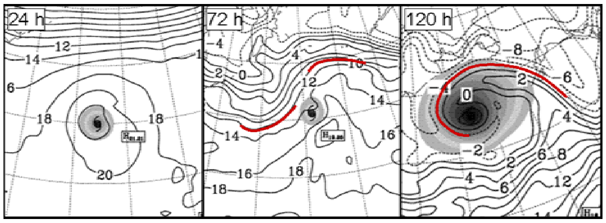

Fig. 5: *850 mb temperature (contour=2°C) and sea-level pressure (shaded every 4 mb < 1000 mb) within the region indicated by the boxes in Fig. 4 for the intensifying case: a) 24 h; b) end of stage 1; and c) end of stage 2. Frontal zones are indicated with thick red lines.*

the convective term in the simulation (Fig. 6a). By the end of stage 1 (Fig. 6b), the precipitation is mostly due to the explicit cloud scheme and is concentrated in a long arc extending from the tropical cyclone center to the northeast along the warm frontal zone shown in Fig. 5b. Note that very little precipitation is associated with the weak cold front that extends to the west of the tropical cyclone center in Fig. 5b. This seems to be typical of cases in which the tropical cyclone circulation is providing the mechanism for deformation of the baroclinic zone (e.g., Klein et al. 2000). Near the tropical cyclone center, the majority of the precipitation at the end of stage 1 (Fig. 6b) lies in the inner portion of the northwest quadrant and the

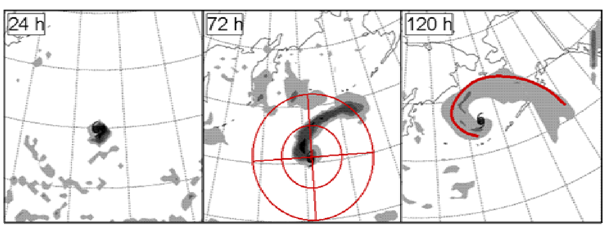

Fig. 6: *Six-hourly precipitation (shading > 1 mm/6h, contours 1, 5, 10, 25, 50 mm/6h) within the region indicated by the boxes in Fig. 4 for the intensifying case: a) 24 h; b) end of stage 1; and c) end of stage 2. The circle quadrants in b) indicate the inner and outer quadrant areas that are used to calculate forecast parameters in section 5.*

outer portion of the northeast quadrant, which is typical of the re-intensifying cases and is due to the development of precipitation along the warm front from upslope mechanics (Ritchie and Elsberry 2003). At the end of stage 2 (Fig. 6c), the precipitation has weakened and is concentrated in a spiral band that extends to the northeast from the cyclone center in a typical occluding configuration.

4.2 Dissipators – Case 25S15E

The 500-mb geopotential height and sea-level pressure patterns are presented in Fig. 7 at key stages in the life cycle of a dissipating extratropical transition simulation. Similar to the re-intensifying case, the midlatitude trough and the tropical cyclone are initially distinct features in the 500-mb height and surface pressure fields (compare Figs. 4a, 7a). Prior to 120 h of integration, the tropical cyclone weakens considerably as it approaches the midlatitude baroclinic zone (Fig. 2). By 120 h (Fig. 7b), the tropical cyclone has become embedded as an open wave on the strong zonal flow that marks the baroclinic zone and has filled to a sea-level pressure of 1012 mb (Fig. 2). We consider this open wave pattern as the end of stage 1 of extratropical transition for a dissipating case. Because the midlatitude trough that was almost directly north of the tropical cyclone in Fig. 7a has moved well to the east of the tropical cyclone in Fig. 7b, no interaction leading to extratropical cyclone development is possible. By 168 h (Fig. 7c), the tropical cyclone remnants have continued to dissipate until it is barely identifiable as a weak low pressure system.

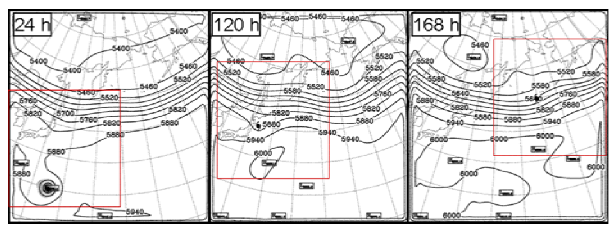

Fig. 7: *500-mb geopotential height field (contour=60 m) and sea-level pressure (shaded every 4 mb < 1000 mb) for the dissipating case: a) 24 h; b) end of stage 1 (120 h); and c) 168 h. The boxes indicate the domains for Fig. 8.*

The 850-mb temperature maps that correspond to Fig. 7 are not presented here. The strong temperature gradient associated with the baroclinic zone is well to the north of the tropical cyclone and the thermal trough associated with the midlatitude trough is located almost directly to the north of the tropical cyclone. By the end of stage 1 of extratropical transition for this simulation, the tropical cyclone has moved northward to the edge of the baroclinic zone. However, the tropical cyclone remnants are so weak that only a slight distortion of the zonally oriented baroclinic zone is produced and minimal frontal development is associated with the distortion (not shown). By 168 h of integration, the tropical cyclone remnants are no longer discernable in the low-level temperature fields.

The 6-hourly precipitation maps that correspond to the boxed domains in Fig. 7 are presented in Fig. 8. Initially (Fig. 8a), the precipitation is concentrated around the tropical cyclone center. By the end of stage 1 (Fig. 8b), the precipitation is concentrated in two regions: a weak region near the rapidly weakening tropical cyclone, and a broader region with the majority of the precipitation to in the outer northeast quadrant of the tropical cyclone associated with the midlatitude trough, which has advected eastward past the tropical cyclone. This precipitation pattern is typical of the dissipating cases if the upper-level trough has advected to the east of the tropical cyclone remnants (e.g., Ritchie and Elsberry 2003). In contrast to the intensifying cases, which have a predictable pattern of precipitation as the trough and tropical cyclone become phased, more or less precipitation may occur in the northeast quadrant for the dissipating cases depending on how far to the east the trough has advected. When the tropical cyclone has dissipated (Fig. 8c), the only precipitation is associated with a weak upper-level trough (Fig. 7c), which may have developed *in situ* with the dissipating tropical cyclone.

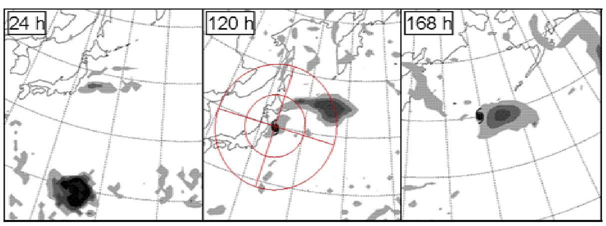

Fig. 8: *Six-hourly precipitation (shading > 1 mm/6h, contours 1, 5, 10, 25, 50 mm/6h) within the region indicated by the boxes in Fig. 7 for the dissipating case: a) 24 h; b) end of stage 1 (120 h); and c) 168 h.*

5. A DISCRIMINATING PARAMETER

Because clear differences are simulated in the spatial patterns of certain parameters (e.g., precipitation) depending on whether the tropical cyclone is dissipating or reintensifying, time series of those parameters are constructed to detect these differences ahead of the ET time. The region surrounding the tropical cyclone is split into two annuli: an inner annulus defined as the area within 600 km of the tropical cyclone center, and an outer annulus defined as the annulus from 600 – 1200 km from the tropical cyclone center. These areas are further split into four quadrants; NE, NW, SW, and SE quadrants (e.g., Figs. 6b, 8b).

Time series of several parameters including 500-mb PVA, 925-mb temperature advection, 250-mb divergence, and precipitation are constructed relative to the end of stage 1. This is defined as the time of maximum sea-level pressure prior to re-intensification, or as the time (to the nearest 6 h) when the tropical cyclone becomes an open wave in the 500-mb geopotential height field for the dissipating cases. The end of Stage 2 is defined as the time of minimum sea-level pressure for the reintensifying cases, and does not apply to the dissipating cases. All reintensifying cases (Fig. 2) are plotted on one axis and all dissipating cases on a second axis and the time series of northwest precipitation are shown in Fig. 9.

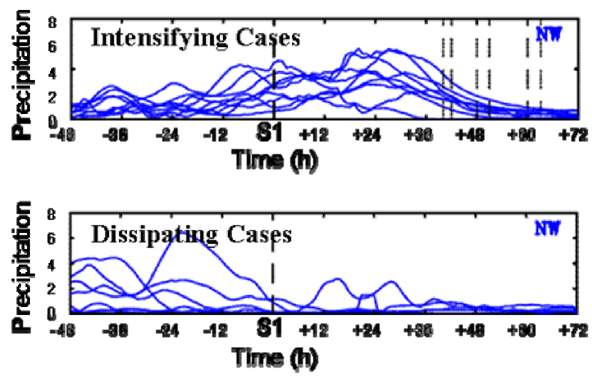

Fig. 9: *Time series of precipitation in the inner northwest quadrant for intensifying (top row) and dissipating (bottom row) cases adjusted in time relative to the time that stage 1 (S1) is completed. Times of the end of stage 2 are indicated by dashed vertical lines for the intensifying cases.*

A clear difference exists between the intensifying and dissipating cases in Fig. 9. Evaluation of the northwest quadrant, inner-radius precipitation reveals a general rising trend prior to the end of stage 1 to a value of greater than 0.6 mm/6h for intensifying cases versus a decreasing or stable weak trend of less than 0.6 mm/6h for the dissipating cases. This characteristic correctly identifies all cases as either intensifying or dissipating (Table 1).

From the parameters investigated thus far, eleven discriminating factors can be discerned prior to the end of Stage 1 of ET (bold parameters in Tables 1 and 2). These include the patterns of 500-mb PVA in the inner northeast and northwest quadrants, 200-mb divergence in the inner northwest quadrant, precipitation in the inner northeast and northwest quadrants, and the pattern of low-level temperature advection in all inner quadrants, and the pattern of low-level

Inner radius 0-600 km (per unit area)		
	I	D
NE PVA > 30 x 10^{-10} s^{-2}	**100%**	**14%**
NE T advection weakly rising to > 7 x 10^{-5} K s^{-1}	**100%**	**17%**
NE Divergence weakly rising to > 1.2 x 10^{-5} s^{-1}	86%	57%
NE Precipitation rising to 2.3 mm/6h at S1	**89%**	**29%**
NW PVA rising > 5 x 10^{-10} s^{-2}	**100%**	**0%**
NW T advection rising to > 7.8 x 10^{-10} K s^{-2}	**100%**	**17%**
NW T advection peaks prior to S1	**86%**	**17%**
NW Divergence > 0.9 x 10^{-5} s^{-1}	**86%**	**0%**
NW Precipitation rising to > 0.6 mm/6h	**100%**	**0%**
SW T advection rising to > 11.1 x 10^{-5} K s^{-1}	**86%**	**0%**
SE T advection rising to > 5.8 x 10^{-5} K s^{-1}	**100%**	**0%**

Table 1: *Percentage of intensifier cases (dissipators) correctly (incorrectly) identified by trends in selected parameters in the inner radius prior to the end of stage 1 of ET. Significant differences in the correct detections of intensifiers versus false detection of dissipators are in bold.*

Outer radius 600-1200 km (per unit area)		
	I	D
NE T advection rising to > 5.2 10^{-5} K s^{-1}	71%	33%
NE Precipitation > 0.3 mm/6h	100%	57%
NW Precipitation > 0.2 mm/6h	33%	0%
SW T advection > 3.0 10^{-5} K s^{-1}	**100%**	**17%**

Table 2: *Similar to Table 1 except for threshold parameters in the outer-radius prior to the end of stage 1 of ET. Significant differences in the correct detections of intensifiers versus false detection of dissipators are in bold.*

temperature advection in the outer southwest quadrant of the tropical cyclone.

A physical interpretation based on the Petterssen Type B conceptual model is that the re-intensifying cases would be experiencing amplification and distortion of the baroclinic zone due to warm advection to the NE and cold advection to the SW in conjunction with 500-mb positive vorticity advection in advance of a trough that is tilted westward with elevation due to the cold advection on the west side. Such a trough position is consistent with 200 mb divergence in the northwest quadrant and precipitation in the northeast quadrant. Klein et al. (2000) and many others have identified the development of asymmetric precipitation with a maximum in the northeast quadrant as typical of extratropical transition in the western North Pacific region.

Inner radius 0-600 km (per unit area)		
	I	D
NE PVA > 30 x 10^{-10} s^{-2} for > 12 h	**100%**	**0%**
NE T advection > 10 x 10^{-5} K s^{-1} for 12 h	**100%**	**17%**
NE Precipitation peaks at > 4.0 mm/6h in 30 h	**100%**	**14%**
NW PVA > 10 x 10^{-10} s^{-2} for > 12 h	**100%**	**0%**
NW Divergence peaks at > 1.8 x 10^{-5} s^{-1} in 24 h	**100%**	**14%**
NW Precipitation peaks at > 2.0 mm/6h in 36 h	**100%**	**14%**
SW T advection peaks at > 20 x 10^{-5} K s^{-1} within 24 h	**86%**	**0%**
SE PVA > 20 10^{-10} s^{-2} for > 12 h	57%	17%
SE T advection peaks at > 15 x 10^{-5} K s^{-1} within 24 h	**100%**	**17%**

Table 3: *Similar to Table 1 except for stage 2 of ET.*

Much stronger signals are present in the stage 2 (reintensification) parameters (bold in Tables 3 and 4). For example, the strong peaks of 850-mb temperature advection in the northeast and southeast quadrants in both the inner and outer radius are clearly different for the intensifying cases than for the dissipating cases and correctly identify all intensifying cases while only incorrectly identifying one dissipating case. However, these parameters change along with an already falling sea-level pressure and thus are not of predictive use.

The best use of these parameters would be to combine them into a single parameter that indicates whether intensification will or will not occur for any given case of extratropical transition. Work in progress for developing this parameter will involve: 1) extending the number of simulated cases to 48 to include variations in the trough structure; and 2) examining real cases using analyses of all the distinguishing parameters for individual cases to validate their usefulness in distinguishing intensifying and dissipating cases An example comparison of the intensifying and

Outer radius 600-1200 km (per unit area)	I	D
NE T advection peaks at > 10.0 x 10^{-5} K s^{-1} in 24 h	**100%**	**0%**
NE Precipitation > 0.8 mm/6h within 36 h	89%	43%
NW Precipitation > 0.23 mm/6h within 48 h	89%	43%
SW T advection peaks at > 5.0 x 10^{-5} K s^{-1} in 24 h	**100%**	**0%**
SE T advection peaks at > 9.0 x 10^{-5} K s^{-1} in 36 h	**100%**	**0%**

Table 4: As for Table 2 except for *stage 2 of ET.*

dissipating cases discussed in the previous section, with values that are normalized based on a maximum observed value for each parameter is shown in Fig. 10. There is a clear difference between the two cases with an upward trend to over 0.4 units at the end of S1 for the intensifying case when compared to the dissipating case.

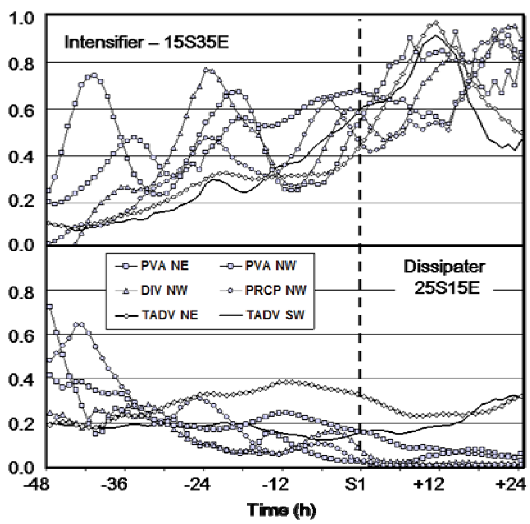

Fig. 10: *Six normalized parameters prior to the end of stage 1 of ET for the two cases discussed in section 4. Open symbols are used for the inner radius parameters and thick solid line for the outer radius parameter. Note the generally higher values and upward trends prior to S1 for the intensifying case versus the dissipating case.*

6. SUMMARY AND CONCLUSIONS

Sixteen idealized simulations are used to explore the effects of different phasing between the midlatitude trough and tropical cyclone during extratropical transition. A consistent spatial pattern of strong, moderate, weak re-intensification or dissipation is simulated. Those cases where the tropical cyclone is initially closest (within 15º latitude) to the baroclinic zone and midlatitude trough develop the deepest cyclones and those farthest away (25º south of the trough) are more likely to dissipate or only weakly re-intensify. The differences in the interaction between the midlatitude trough and tropical cyclone in these idealized simulations can be related to the phasing of the two systems. Whereas Ritchie and Elsberry (2003) found that the strength of the midlatitude trough had little to do with the final intensity of the transitioned cyclone, these simulations indicate the final intensity is extremely sensitive to the initial locations of the two weather systems relative to each other. Clearly, the main forecasting challenge will be to accurately predict the system positions and the timing and magnitude of the interaction. Considering the uncertainty in the initial conditions for both systems, and the subtropical ridge that is bringing the tropical cyclone poleward, and the nonlinearity of the interaction this will be a challenging forecast.

Threshold values of various parameters ahead of the end of stage 1 have been identified as being important in distinguishing whether the system was going to re-intensify or dissipate. Parameters that discriminated between intensifying and dissipating cases of ET *prior to the end of the transformation stage 1* include the inner-radius parameters: NE quadrant PVA, NW quadrant PVA, NW quadrant upper-level divergence, NE quadrant precipitation, NW quadrant precipitation, and all quadrants low-level temperature advection; and the outer-radius parameter: SW quadrant low-level temperature advection. The time series of these parameters in these simulations suggest a capability to discriminate between intensifying and dissipating cases of extratropical transition. However, the caveat is that these parameters have been derived from controlled simulations of ET and their utility in a real forecast situation using operational analyses still needs to be tested.

Future work includes expanding the set of 16 simulations to include the strong and weak trough cases from Ritchie and Elsberry (2003) as well as varying the translation speed, strength, and size of the tropical cyclone. In addition, the utility of the time series parameters for forecasting will be investigated using analysis fields.

Acknowledgments: The COAMPS model was made available by the Naval Research Laboratory, Monterey, CA. All simulations were run at the Center for High Performance Computing at UNM. This research was sponsored by the Office of Naval Research Marine Meteorology Program.

REFERENCES

Deardorff, J. W., 1980: Stratocumulus-capped mixed layers derived from a three-dimensional model. *Bound.-Layer Meteor.,* **18,** 495-527.

DiMego, M., and L. F. Bosart, 1982: The transformation of tropical storm Agnes into an extratropical cyclone. Part I: The observed fields and vertical motion computations. *Mon. Wea. Rev.,* **110**, 385-411.

Foley, G. R., and B. N. Hanstrum, 1994: The capture of tropical cyclones by cold fronts off the west coast of Australia. *Wea. Forecasting,* **9,** 577-592.

Harr, P. A., and R. L. Elsberry, 2000: Extratropical transition of tropical cyclones over the western North Pacific. Part I: Evolution of structural characteristics during the transition process. *Mon. Wea. Rev.,* **128**, 2613–2633.

Harr, P. A., R. L. Elsberry, and T. F. Hogan, 2000: Extratropical transition of tropical cyclones over the western North Pacific. Part II: The impact of midlatitude circulation characteristics. *Mon. Wea. Rev*., **128**, 2634–2653.

Harshvardhan, R. Davies, D. Randall, and T. Corsetti, 1987: A fast radiation parameterization for atmospheric circulation models. *J. Geophys. Res.,* **92,** 1009-1015.

Hodur, R. M., 1997: The Naval Research Laboratory's Coupled Ocean/Atmosphere Mesoscale Prediction System (COAMPS). *Mon. Wea. Rev.,* **125,** 1414-1430.

Kain, J., and J. M. Fritsch, 1993: Convective parameterization for mesoscale models: The Kain-Fritsch scheme. *The Representation of Cumulus Convection in Numerical Models, Meteor. Monogr., No. 46,* American Meteorological Society, Boston, MA 02108, 165-170.

Klein, P. M., P. A. Harr, and R. L. Elsberry, 2000: Extratropical transition of western North Pacific tropical cyclones: An overview and conceptual model of the transformation stage. *Wea. and Forecasting*, **15,** 373-395*.*

Klein, P. M., P. A. Harr, and R. L. Elsberry, 2002: Extratropical transition of western North Pacific tropical cyclones: Midlatitude contributions to intensification. *Mon. Wea. Rev.,* **130,** 2240-2259.

McBride, J. L., and R. M. Zehr, 1981: Observational analysis of tropical cyclone formation. Part II: Comparison of non-developing versus developing systems. *J. Atmos. Sci.,* **38,** 1132-1151.

McTaggart-Cowan, R., J. R. Gyakum, and M. K. Yau, 2001: Sensitivity testing of extratropical transitions using potential vorticity inversions to modify initial conditions: Hurricane Earl case study. *Mon. Wea. Rev.,* **129**, 1617-1636.

Perkey, D. J., and C. W. Krietzberg, 1976: A time-dependent lateral boundary scheme for limited-area primitive equation models. *Mon. Wea. Rev.,* **104**, 744-755.

Petterssen, S., 1956: *Weather Analysis and Forecasting,* 2nd ed., Vol I, McGraw-Hill, New York, NY, 428 pp.

Petterssen, S., and S. J. Smebye, 1971: On the development of extratropical cyclones. *Quart. J. Roy. Meteor. Soc.,* **97**, 457-482.

Ritchie, E. A., and R. L. Elsberry, 2001: Simulations of the transformation stage of the extratropical transition of tropical cyclones. *Mon. Wea. Rev.,* **129,** 1462-1480*.*

Ritchie, E. A., and Elsberry, R. L., 2003: Simulations of the extratropical transition of tropical cyclones: Contributions by the midlatitude upper-level trough to re-intensification. *Mon. Wea. Rev.*, **131**, 2112-2128.

Ritchie, E. A., and Elsberry, R. L., 2005: Simulations of the extratropical transition of tropical cyclones: Phasing between the upper-level trough and tropical cyclone. *Mon. Wea. Rev. submitted*.

Rutledge, S. A., and P. V. Hobbs, 1983: The mesoscale and microscale structure of organization of clouds and precipitation in midlatitude cyclones. VIII: A model for the "seeder-feeder" process in warm-frontal rainbands. *J. Atmos. Sci.,* **40,** 1185-1206.

Sinclair, M. R., 1993: Synoptic-scale diagnosis of the extratropical transition of a southwest Pacific tropical cyclone. *Mon. Wea. Rev.,* **121**, 941-960.